J|A|C|S
ARTICLES
Published on Web 10/15/2002

Donor/Acceptor Interactions in Systematically Modified $Ru^{II}-Os^{II}$ Oligonucleotides

Dennis J. Hurley and Yitzhak Tor*

Contribution from the Department of Chemistry and Biochemistry, University of California, San Diego, La Jolla, California 92093-0358

Received February 4, 2002

Abstract: Donor/acceptor (D/A) interactions are studied in a series of doubly modified 19-mer DNA duplexes. An ethynyl-linked Ru^{II} donor nucleoside is maintained at the 5′ terminus of each duplex, while an ethynyl-linked Os^{II} nucleoside, placed on the complementary strands, is systematically moved toward the other terminus in three base pair increments. The steady-state Ru^{II}-based luminescence quenching decreases from 90% at the shortest separation of 16 Å (3 base pairs) to ~11% at the largest separation of 61 Å (18 base pairs). Time-resolved experiments show a similar trend for the Ru^{II} excited-state lifetime, and the decrease in the averaged excited-state lifetime for each duplex is linearly correlated with the fraction quenched obtained by steady-state measurements. Analysis according to the Förster dipole−dipole energy transfer mechanism shows a reasonable agreement. Deviation from idealized behavior is primarily attributed to uncertainty in the orientation factor, κ^2. Analyzing D/A interactions in an analogous series of doubly modified oligonucleotides, where the ethynyl-linked Ru^{II} center is replaced with a saturated two-carbon linked complex, yields an excellent correlation with the Förster mechanism. As this simple change partially relaxes the rigid geometry of the donor chromophore, these results suggest that the deviation from idealized Förster behavior observed for the duplexes containing the rigidly held Ru^{II} center originates, at least partially, from ambiguities in the orientation factor. Surprisingly, analyzing both quenching data sets according to the Dexter mechanism also shows an excellent correlation. Although this can be interpreted as strong evidence for a Dexter triplet energy transfer mechanism, it does not imply that this electron exchange mechanism is operative in these D/A duplexes. Rather, it suggests that systems that transfer energy via the Förster mechanism can under certain circumstances exhibit Dexter-like "behavior", thus illustrating the danger of imposing a single physical model to describe D/A interactions in such complex systems. While we conclude that the Förster dipole−dipole energy transfer mechanism is the dominant pathway for D/A interactions in these modified oligonucleotides, a minor contribution from the Dexter electron exchange mechanism at short distances is likely. This complex behavior distinguishes DNA-bridged Ru^{II}/Os^{II} dyads from their corresponding low molecular-weight and covalently attached counterparts.

Introduction

The DNA double helix has been shown to be an intriguing medium for exploring charge transfer phenomena.[1] The intricacies of these processes have widely been probed using photoactive and redox-active transition metal coordination compounds.[2] Much less attention has been given, however, to energy transfer processes in similarly metal-modified DNA oligonucleotides. The relatively complex excited-state manifold of polypyridine Ru^{II} and Os^{II} compounds can be engaged in multiple relaxation mechanisms, including dipole−dipole (Förster) and electron exchange (Dexter) energy transfer processes (Figure 1).[3,4] In simple heteronuclear $Ru^{II}-Os^{II}$ dyads, the mode of the donor/acceptor interaction has been demonstrated to be dependent on the ligand bridging the two metal centers.[5] Saturated bridging ligands do not provide effective orbital overlap between donor and acceptor chromophores. Consequently, energy transfer between the photoexcited donor and the ground-state acceptor proceeds primarily by a through-space dipole−dipole interaction.[6] On the other hand, conjugated bridging ligands that provide substantial electronic interaction between the donor and the acceptor can facilitate rapid energy transfer via a through-

* Address correspondence to this author. E-mail: ytor@ucsd.edu.

(1) For overview articles, see: Netzel, T. L. *J. Chem. Educ.* **1997**, *74*, 646−651. Diederichsen, U. *Angew. Chem., Int. Ed. Engl.* **1997**, *36*, 2317−2319. Holmlin, R. E.; Dandliker, P. J.; Barton, J. K. *Angew. Chem., Int. Ed. Engl.* **1997**, *36*, 2714−1730. Netzel, T. L. *J. Biol. Inorg. Chem.* **1998**, *3*, 210−214. Priyadarshy, S.; Risser, S. M.; Beratan, D. N. *J. Biol. Inorg. Chem.* **1998**, *3*, 196−200. Erkkila, K. E.; Odom, D. T.; Barton, J. K. *Chem. Rev.* **1999**, *99*, 2777−2795. Grinstaff, M. W. *Angew. Chem., Int. Ed.* **1999**, *38*, 3629−3635. Schuster, G. B. *Acc. Chem. Res.* **2000**, *33*, 253−260. Núñez, M. E.; Barton, J. K. *Curr. Opin. Chem. Biol.* **2000**, *4*, 199−206.

(2) Murphy, C. J.; Arkin, M. R.; Jenkins, Y.; Ghatlia, N. D.; Bossmann, S. H.; Turro, N. J.; Barton, J. K. *Science* **1993**, *262*, 1025−1029. Meade, T. J.; Kayyem, J. F. *Angew. Chem., Int. Ed. Engl.* **1995**, *34*, 352−354. Arkin, M. R.; Stemp, E. D. A.; Holmlin, R. E.; Barton, J. K.; Hörmann, A.; Olson, E. J. C.; Barbara, P. F. *Science* **1996**, *273*, 475−480. Dandliker, P. J.; Holmlin, R. E.; Barton, J. K. *Science* **1997**, *275*, 1465−1468. Ortmans, I.; Content, S.; Boutonnet, N.; Kirsch-De Mesmaeker, A.; Bannwarth, W.; Constant, J.-F.; Defrancq, E.; Lhomme, J. *Chem.−Eur. J.* **1999**, *5*, 2712−2721. Núñez, M. E.; Hall, D. B.; Barton, J. K. *Chem. Biol.* **1999**, *6*, 85−97. Rack, J. J.; Krider, E. S.; Meade, T. J. *J. Am. Chem. Soc.* **2000**, *122*, 6287−6288. Tierney, M. T.; Sykora, M.; Khan, S. I.; Grinstaff, M. W. *J. Phys. Chem. B* **2000**, *104*, 7574−7576. Stemp, E. D. A.; Holmlin, R. E.; Barton, J. K. *Inorg. Chim. Acta* **2000**, *297*, 88−97. Schiemann, O.; Turro, N. J.; Barton, J. K. *J. Phys. Chem. B* **2000**, *104*, 7214−7220. Williams, T. T.; Odom, D. T.; Barton, J. K. *J. Am. Chem. Soc.* **2000**, *122*, 9048−9049.

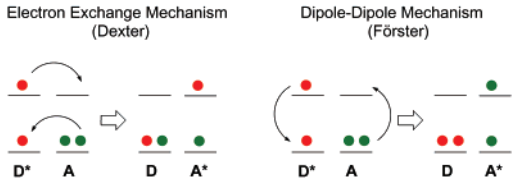

Figure 1. Schematic representation of two possible energy transfer mechanisms between Ru^{II} and Os^{II} metal complexes. The Dexter mechanism involves an electron exchange process, while the Förster mechanism involves a nonradiative and indirect Coulombic dipole−dipole interaction.

bond Dexter exchange mechanism.[7,8] How would DNA mediate donor/acceptor interactions in related duplex-bridged Ru^{II}−Os^{II} dyads?

Barton has previously investigated DNA-mediated triplet energy transfer using end-intercalating dimethyl-dppz Ru^{II} and Os^{II} metal complexes.[9] A shallow distance dependency was observed over a relatively narrow donor/acceptor (D/A) separation of 31−44 Å. The sensitivity of the observed luminescence quenching to the stacking of the metal complexes and to duplex integrity led the authors to conclude that triplet energy transfer is effectively mediated by the DNA base stack. Since triplet energy transfer can be viewed as a charge transfer process, where concerted hole and electron transfer processes take place (Figure 1),[10,11] these results have been interpreted using the Dexter exchange mechanism. This mechanism, however, requires orbital overlap and operates at relatively short distances.[12] The significant quenching observed at distances above 30 Å may require reinterpretation.

We have previously developed an effective method for the site-specific incorporation of polypyridine Ru^{II} and Os^{II} complexes into DNA oligonucleotides using solid-phase phosphoramidite chemistry.[13,14] In our novel nucleosides, a $[(bpy)_2M$-(3-ethynyl-1,10-phenanthroline)$]^{2+}$ complex is covalently attached to the 5-position of 2′-deoxyuridine and projected into the DNA major groove (Figure 2). The rigid ethynyl linker that connects the polypyridine moiety to the heterocyclic base ensures that the metal complexes do not back-intercalate into the duplex, and an unambiguous positioning of the donor and the acceptor.[15] In this contribution, DNA-bridged Ru^{II}−Os^{II} dyads, where the donor/acceptor separation is systematically varied from three to eighteen base pairs, are investigated. To minimize perturbations, a single DNA sequence is utilized and only the internal positioning of the acceptor is varied. A series of six doubly modified duplexes that contain the Ru^{II} donor **1a** and Os^{II} acceptor **1b** is investigated and compared to an analogous series, where the donor nucleoside **1a** is replaced with **2** (Figure 2). Steady-state and time-resolved experiments reveal a complex distance dependent behavior. The participation of both the Förster and Dexter mechanisms in the transmission of excited-state energy across the DNA bridge is analyzed.

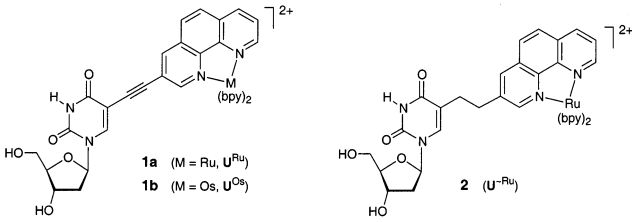

Figure 2. Structures of the ethynyl-linked Ru^{II}- and Os^{II}-containing nucleosides **1a** and **1b**, respectively, and the "saturated" dimethylene-linked Ru^{II} nucleoside **2**.

Results and Discussion

Duplex Design and Synthesis. To systematically study the interaction between a Ru^{II} donor nucleoside **1a** and an Os^{II}-containing acceptor nucleoside **1b** over a DNA bridge, a series of six doubly modified 19-mer DNA duplexes has been designed. A single Ru^{II} nucleoside is maintained at the 5′ terminus of each duplex, while the Os^{II} nucleoside, placed on the complementary strands, is systematically moved toward the other terminus in three base pair increments (Figure 3). The donor/acceptor separation spanned in this series is from 16 to above 60 Å. Figure 3 lists "duplex codes" which describe the modified duplexes in a concise manner, indicating the positioning of the acceptor with respect to the donor. For example, $U^{Ru}(19)\cdot U^{Os}(4)$ refers to duplex **5·6**, where the donor strand is modified at the 19th (terminal) position from the 3′-end with the Ru^{II}-modified deoxyuridine **1a**, while the complementary strand is modified at the 4th position with the Os^{II} nucleoside **1b**.

All metal-containing oligonucleotides were synthesized with the epimeric (Λ/Δ) metal-containing D-ribose phosphoramidites, utilizing standard solid-phase DNA synthesis.[16] As previously reported, the coupling efficiency of the metal-containing phosphoramidites during DNA synthesis can be greater than 90% when high reagent purity is maintained.[14] The 5′-DMT protected oligonucleotides were treated with ammonia and purified by reverse-phase HPLC. After deprotection using 80% acetic acid,

(3) (a) Juris, A.; Balzani, V.; Barigelletti, F.; Campagna, S.; Belser, P.; Von Zelewsky, A. *Coord. Chem. Rev.* **1988**, *84*, 85−277. (b) Sauvage, J.-P.; Collin, J.-P.; Chambron, J.-C.; Guillerez, S.; Coudret, C.; Balzani, V.; Barigelletti, F.; De Cola, L.; Flamigni, L. *Chem. Rev.* **1994**, *94*, 993−1019. (d) Balzani, V.; Juris, A.; Venturi, M.; Campagna, S.; Serroni, S. *Chem. Rev.* **1996**, *96*, 759−833. (e) Barigelletti, F.; Flamigni, L.; Collin, J.-P.; Sauvage, J.-P. *Chem. Commun.* **1997**, 333−338.
(4) For the original formulation of the Förster and Dexter mechanisms, see: (a) Förster, Th. *Discuss. Faraday Soc.* **1959**, *27*, 7−17. (b) Dexter, D. L. *J. Chem. Phys.* **1953**, *21*, 836−850.
(5) For review articles, see: Barigelletti, F.; Flamigni, L. *Chem. Soc. Rev.* **2000**, *29*, 1−12. Ward, M. D.; Barigelletti, F. *Coord. Chem. Rev.* **2001**, *216−217*, 127−154.
(6) Vögtle, F.; Frank, M.; Nieger, M.; Belser, P.; von Zelewsky, A.; Balzani, V.; Barigelletti, F.; De Cola, L.; Flamigni, L. *Angew. Chem., Int. Ed. Engl.* **1993**, *32*, 1643−1646. See also: Belser, P.; Dux, R.; Baak, M.; De Cola, L.; Balzani, V. *Angew. Chem., Int. Ed. Engl.* **1995**, *34*, 595−598.
(7) Representative examples: Groshenny, V.; Harriman, A.; Ziessel, R. *Angew. Chem., Int. Ed. Engl.* **1995**, *34*, 1100−1102. Barigelletti, F.; Flamigni, L.; Guardigli, M.; Juris, A.; Beley, M.; Chodorowski-Kimmes, S.; Collin, J. P.; Sauvage, J. P. *Inorg. Chem.* **1996**, *35*, 136−142. Harriman, A.; Ziessel, R. *Chem. Commun.* **1996**, 1707−1716. Ziessel, R.; Hissler, M.; El-ghayoury, A.; Harriman, A. *Coord. Chem. Rev.* **1998**, *178−180*, 1251−1298. Harriman, A.; Romero, F. M.; Ziessel, R. Benniston, A. C. *J. Phys. Chem. A* **1999**, *103*, 5399−5408. El-ghayoury, A.; Harriman, A.; Khatyr, A.; Ziessel, R. *Angew. Chem., Int. Ed.* **2000**, *39*, 185−189.
(8) Mixed behavior, where both mechanisms are operative, has also been observed. See ref 5 and for example: Groshenny, V.; Harriman, A.; Hissler, M.; Ziessel, R. *J. Chem. Soc., Faraday Trans.* **1996**, *92*, 2223−2238.
(9) Holmlin, R. E.; Tong, R. T.; Barton, J. K. *J. Am. Chem. Soc.* **1998**, *120*, 9724−9725.
(10) Closs, G. L.; Miller, J. R. *Science* **1988**, *240*, 440−447. Closs, G. L.; Johnson, M. D.; Miller, J. R.; Piotrowiak, P. *J. Am. Chem. Soc.* **1989**, *111*, 3751−3753.
(11) Essentially an electron transfer phenomenon, the energy transfer rate is expected to decrease exponentially with increasing D/A separation (R). Thus, the following relationship should hold: $k = A \exp[-\beta R]$.
(12) Turro, N. J. *Modern Molecular Photochemistry*; University Science Books: Sausalito, CA, 1991.
(13) Hurley, D. J.; Tor, Y. *J. Am. Chem. Soc.* **1998**, *120*, 2194−2195.
(14) Hurley, D. J.; Tor, Y. *J. Am. Chem. Soc.* **2002**, *124*, 3749−3762.
(15) The ethynyl linkage also leads to "localization" of the emissive Ru^{II} excited state on the heterocycle-extended nucleoside (see ref 14).
(16) We have previously demonstrated that quenching by the racemic Os^{II} nucleoside **1b** is weakly dependent on the absolute configuration at the Ru^{II} donor metal center (see ref 14).

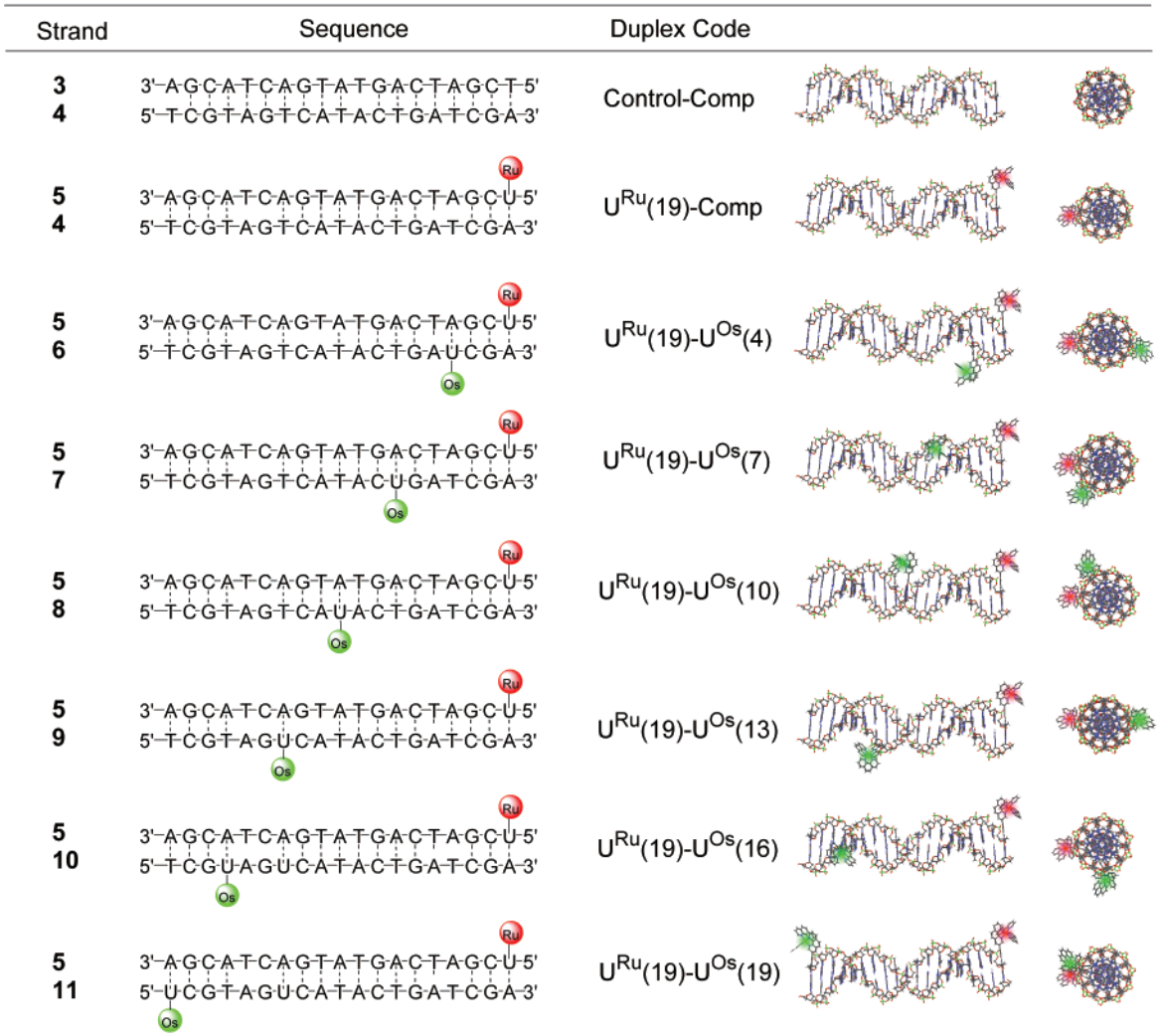

Figure 3. Six doubly metal-modified DNA 19-mer duplexes (**5·6**−**5·11**) contain a single donor Ru^{II} nucleoside **1a** at the 5′-end (red) and an acceptor Os^{II} nucleoside **1b** (green) on the complementary strand. The D/A separation is systematically varied in three base pair increments. Also shown are control oligonucleotides **3·4** and **5·4** and "duplex codes" which describe the duplexes in a concise manner. Models of the doubly modified DNA duplexes are shown on the right. The top view of each duplex emphasizes the angular change between the donor and the acceptor as a function of distance.

HPLC purification was repeated. All oligonucleotides used for the study discussed below were >98% pure by analytical HPLC.[17]

Stability of Doubly Modified Duplexes. Thermal denaturation experiments have been used to determine the stability of the modified DNA duplexes. Complementary combinations of metal-modified oligonucleotides were hybridized in 10 mM phosphate buffer at pH 7.0 containing 100 mM NaCl by slow cooling from 90 °C to either room temperature or 4 °C. The dissociation of each duplex was monitored at 260 nm as a function of temperature. The T_m values of the control and the modified duplexes are summarized in Table 1. The presence of a metal-containing nucleotide, at a terminal or internal position, has a minimal effect on duplex stability. The impact of the modification is dependent on the location of the metal-containing nucleotide within the sequence. Modification at the end of the duplex, as seen in the 19-mer duplexes U^{Ru}(19)·Comp **5·4** and U^{Ru}(19)·U^{Os}(19) **5·11**, results in a slight increase in duplex stability ($\Delta T_m = +0.7$ and $+0.2$ °C, respectively) relative to that of the unmodified control 19-mer duplex **3·4** ($T_m = 62.0$ °C). The incorporation of an Os^{II} nucleoside to the complementary strand at an internal position results in a minimal decrease in duplex stability ($\Delta T_m \cong -1$ °C), except in duplex U^{Ru}(19)·U^{Os}(10) **5·8**, where a small increase in T_m is observed relative to the control duplex.

Steady-State Luminescence Quenching Experiments. The steady-state transfer efficiency at each of the six donor/acceptor separations was determined by comparing the integrated emission between 525 and 850 nm of each duplex with that of the U^{Ru}(19)·Comp control duplex **5·4** (Figure 4).[18,19] The results are presented in Table 1 as the fraction quenched at each distance.[20] The level of Ru^{II}-based luminescence quenching

(17) Enzymatic digestion using a cocktail of nuclease P1, alkaline phosphatase, and snake venom phosphodiesterase was used to confirm both the integrity of the incorporated metal-containing nucleoside and the composition of the modified oligonucleotide strands. See Supporting Information for experimental details and data. The metal-modified oligonucleotides were also characterized by MALDI mass spectrometry. For example, the MS data for the Ru^{II}-modified oligonucleotide **5**: calcd 6429.5 Da, found 6423 ± 6 Da . The MS data of the Os^{II}-modified oligonucleotides **6**−**11**: calcd 6509.6 Da, found 6510 ± 6 Da.

(18) Excitation of the Ru-only control and bis(heterometalated) duplexes was performed at 467 nm, an isosbestic point in the absorption spectrum of the Ru^{II} and Os^{II} nucleosides.

Table 1. Thermal Denaturation, Steady-State Luminescence Quenching, and Excited-State Lifetimes of DNA Duplexes Containing an Ethynyl-Linked Ru^{II} Donor **1a** and an Ethynyl-linked Os^{II} Acceptor **1b**[a]

duplex	duplex code	T_m[b] (°C)	ΔT_m[c] (°C)	D/A distance[d] (Å)	fraction quenched[e]	$\tau 1$ μs[f] (%)	$\tau 2$ μs[f] (%)	$\langle\tau\rangle$ μs[g]	decrease in $\langle\tau\rangle$ (%)
3·4	control·Comp	62.0							
5·4	U^{Ru}(19)·Comp	62.7	+0.7			1.74(44)	1.03(56)	1.31 ± 0.01	
5·6	U^{Ru}(19)·U^{Os}(4)	61.0	−1.0	16	0.89 ± 0.01	1.075(16)	0.037(84)	0.20 ± 0.06	85
5·7	U^{Ru}(19)·U^{Os}(7)	59.9	−1.1	21	0.80 ± 0.01	0.960(18)	0.120(82)	0.27 ± 0.01	79
5·8	U^{Ru}(19)·U^{Os}(10)	62.7	+0.7	31	0.57 ± 0.01	0.895(63)	0.345(37)	0.63 ± 0.01	52
5·9	U^{Ru}(19)·U^{Os}(13)	61.0	−1.0	43	0.29 ± 0.03	1.535(39)	0.745(61)	1.02 ± 0.12	22
5·10	U^{Ru}(19)·U^{Os}(16)	62.0	0.0	52	0.14 ± 0.03	1.820(28)	1.05(72)	1.24 ± 0.02	5
5·11	U^{Ru}(19)·U^{Os}(19)	62.2	+0.2	61	0.11 ± 0.03	3.815(5)	1.19(95)	1.27 ± 0.01	3

[a] All measurements were performed with 2 μM duplex solutions in 100 mM NaCl, 10 mM phosphate buffer at pH 7.0. Steady-state and time-resolved luminescence experiments were done with deoxygenated solutions.[18,19] [b] Absorbance-derived T_m values were calculated from the derivative of each thermal denaturation curve. Standard deviations are ± 0.5 °C. [c] $\Delta T_m = T_m$(metal-modified duplex) − T_m(control unmodified duplex). [d] Donor/acceptor separations were calculated using a helical DNA model.[26] [e] Fraction quenched: $Fq = 1 - I_{Ru+Os}/I_{Ru}$. The data are the average of three separate determinations. Transfer efficiency was determined by comparing the integrated emission between 525 and 850 nm of each duplex with that of the U^{Ru}(19)·Comp control duplex **5·4**. [f] Samples were excited at 467 nm, and emission decays were monitored at 630 nm. Decays were analyzed according to the biexponential function: $I_{em}(t) = A_1\exp(-t/\tau_1) + A_2\exp(-t/\tau_2)$. [g] Weighted average lifetimes $\langle\tau\rangle$ were calculated by the equation $\langle\tau\rangle = A_1\tau_1 + A_2\tau_2$.

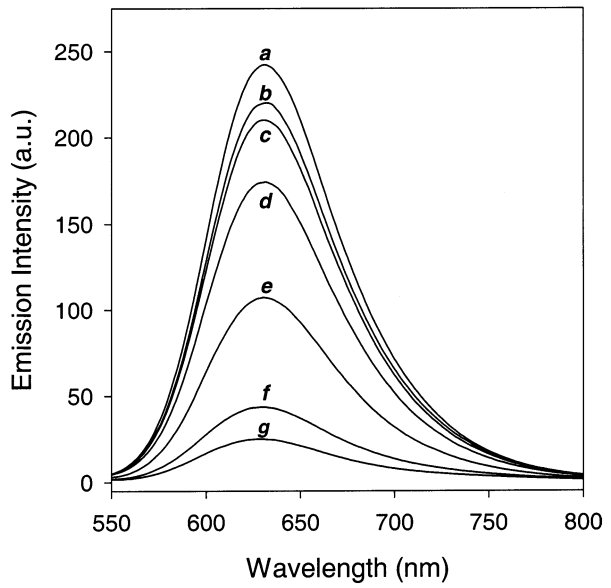

Figure 4. Steady-state emission spectra of the control oligo **5·4** (a) and the D/A oligonucleotides **5·6**−**5·11** (g−b, respectively). See Experimental Section for conditions.

decreases from 90% at the shortest separation of 16 Å (3 base pairs) to ∼11% at the largest separation of 61 Å (18 base pairs).[21]

Control Experiments: Intraduplex Nature of D/A Interactions. To confirm the intraduplex nature of the observed luminescence quenching, three distinct control experiments have been conducted. The interaction of a Ru^{II}-modified duplex U^{Ru}(19)·Comp **5·4** with a soluble, noncovalently attached and non-intercalating $[Os(bpy)_2phen]^{2+}$ was first examined. Figure 5A shows the fraction of Ru^{II} emission quenched as a function of increasing concentrations of Os^{II}. The addition of 1 equiv. of an Os^{II} complex resulted in only 4% intermolecular quenching. It is apparent that the amount of intermolecular quenching is substantially smaller than that observed in the bis(heterometalated) DNA duplexes.[22]

Additional support was obtained by titrating the complementary 19-mer strand U^{Os}(10) **8** into a solution of U^{Ru}(19) 19-mer **5**. The Ru^{II}-based luminescence was monitored at each increment.[23] Importantly, the sample was heated to 90 °C between additions of the complementary oligonucleotide to facilitate duplex rehybridization. Figure 5B plots the fraction of quenched emission as a function of acceptor oligonucleotide concentration. The fraction quenched grows with increasing U^{Os}(10) complement concentration and levels off at 0.59 after the addition of precisely 1 equiv. of the quencher oligonucleotide. A similar 57% luminescence quenching was observed from the direct formation of the same duplex with a 1:1 mixture of U^{Ru}(19) and U^{Os}(10) 19-mer complement (Table 1). It is informative to note that the addition of another full equivalent of U^{Os}(10) oligonucleotide results in only a 4% increase in quenching. This correlates well with the intermolecular quenching for a "soluble" Os^{II} complex discussed above (Figure 5A).

In the last control experiment, the luminescence spectra of the Ru/Os duplex U^{Ru}(19)·U^{Os}(10) **5·8** and the control duplex U^{Ru}(19)·Comp **5·4** were monitored as a function of temperature, starting at 25 °C and ending at 75 °C, well above the melting point of either duplex (T_m = 62.7 °C). Thermal denaturation of the duplex should effectively disrupt any intraduplex D/A interaction. The luminescence of duplex U^{Ru}(19)·Comp **5·4** shows a steady decrease in luminescence intensity with increasing temperature, dropping to 27% of its initial intensity (Figure 6A). This behavior is anticipated, as the emissive properties of polypyridyl Ru^{II} complexes are known to be temperature dependent.[24] The emission profile of the bis(metalated) duplex U^{Ru}(19)·U^{Os}(10) **5·8** shows a similar steady loss in luminescence intensity with increased temperature up to approximately 55 °C (Figure 6B). At this temperature, however, the duplex begins

(19) The luminescence emission resulting from the direct excitation of the acceptor was monitored with the corresponding Os^{II}-only duplex and subtracted from the emission of the donor but was found to be negligible due to the extremely low emission of the Os^{II} nucleoside (see also ref 14).

(20) Distances were calculated using a helical model of the DNA duplex. See Supporting Information for details.

(21) It is important to emphasize that the quenching observed is highly reproducible over several sample preparations and multiple measurements, suggesting minimal photodeterioration of the samples.

(22) Note that a small and constant contribution to quenching (∼5%) in the doubly modified duplexes **5·6**−**5·11** may result from intermolecular interactions, as illustrated for $[Os(bpy)_2phen]^{2+}$ in Figure 5A.

(23) Each measurement was corrected with respect to a control sample to which an equivalent amount of the nonmetalated complement had been added to correct for quenching that resulted simply from duplex formation (see also ref 14).

(24) The emissive ^{3}MLCT state of the metal complex is in thermal equilibrium with an ^{3}MC (metal-centered) level at a slightly higher energy from which the excited state can undergo fast, radiationless decay. Thus, thermally activated crossing into this ^{3}MC level results in reduced Ru^{II} luminescence at higher temperatures. See ref 3a.

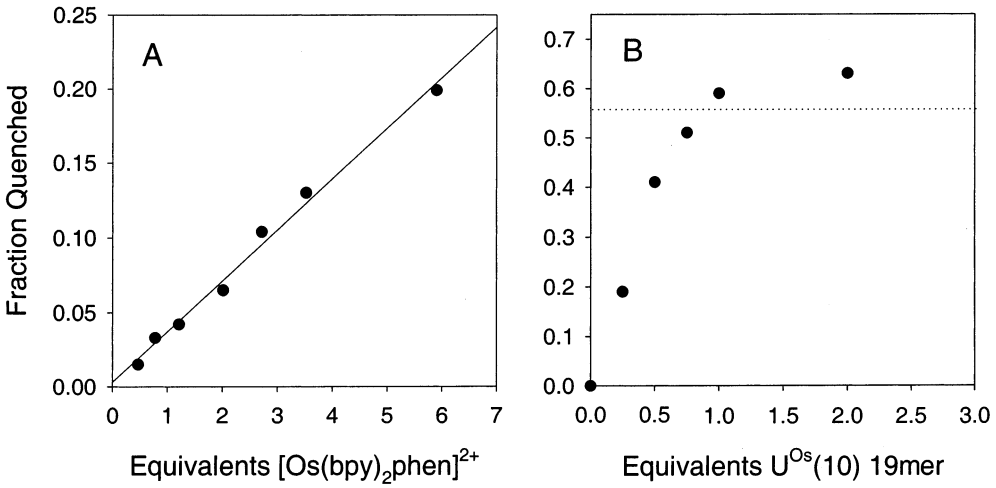

Figure 5. (A) Fraction quenched of the photoexcited duplex $U^{Ru}(19)$·Comp **5·4** in the presence of increasing concentrations of $[Os(bpy)_2phen]^{2+}$ in degassed 100 mM NaCl, 10 mM phosphate buffer at pH 7.0. (B) Fraction quenched of the photoexcited single strand $U^{Ru}(19)$ **5** in the presence of increasing concentrations of complementary strand $U^{Os}(10)$ **8** (2 μM in 100 mM NaCl, 10 mM phosphate buffer at pH 7.0). Dashed line represents the 0.57 threshold.

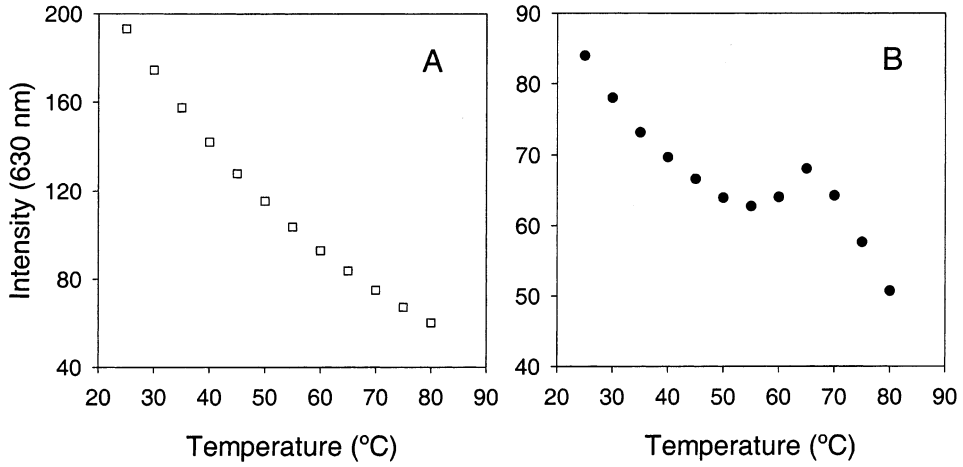

Figure 6. Emission of the control $U^{Ru}(19)$·Comp **5·4** duplex (A) and $U^{Ru}(19)$·$U^{Os}(10)$ duplex **5·8** (B) as a function of temperature (2 μM air equilibrated samples in 100 mM NaCl, 10 mM phosphate buffer at pH 7.0).

to thermally denature and the donor/acceptor distance increases. This leads to emission enhancement that peaks at around 65 °C. A further increase in temperature results in decreased emission, resulting from thermal deactivation of the Ru^{II} excited state. It is worth noting that the "melting temperature" obtained from the temperature-dependent luminescence (~60 °C) agrees well with the T_m obtained by monitoring the absorption of the duplex at 260 nm as a function of temperature (62.7 °C). When taken together, we conclude that the Ru^{II} emission quenching observed in duplexes **5·6**−**5·11** represents an intraduplex event.[25]

Time-Resolved Luminescence Experiments. The donor excited-state lifetimes in the metal-modified duplexes were measured by monitoring the decay of the Ru^{II}-based emission at 630 nm (Figure 7 and Table 1). While the decay of the free Ru^{II} nucleoside **1a** is monoexponential with an excited-state lifetime of 1.13 μs in aqueous solutions, incorporation of the nucleoside into DNA (single or double stranded) results in a biexponential decay.[14] The decays are characterized by a longer-lived component (τ1), accompanied by a shorter lived decay (τ2). The weighted average lifetime $\langle\tau\rangle$ of the $U^{Ru}(19)$·Comp duplex is 1.31 μs, slightly longer than the monoexponential 1.13 μs lifetime of the free nucleoside (Table 1). The increased lifetime is likely a result of partial protection of the Ru^{II} complex from the aqueous environment and is characterized by nearly equal distribution between a longer-lived excited state (1.74 μs) and a slightly shorter-lived excited state (1.03 μs).[14] In the heterometalated duplexes, the closer the Os^{II} quencher is to the Ru^{II} complex, the shorter the averaged Ru^{II} excited-state lifetime $\langle\tau\rangle$ (Table 1).[26] Very importantly, the decrease in the averaged excited-state lifetime for each duplex is linearly correlated with

(25) Detecting the sensitization of Os^{II} emission would have provided an additional support for an energy transfer process (vs, for example, a reductive quenching). This has been found to be technically challenging because of the low emission quantum yield of the Os^{II} nucleoside **1b** (Φ < 0.0001).[14] Following a procedure analogous to that used by Clegg (Clegg, R. M.; Murchie, A. I.; Zechel, A.; Lilley, D. M. *Proc. Natl. Acad. Sci. U.S.A.* **1993**, *90*, 2994−2998), one can subtract a normalized donor signal from the donor/acceptor luminescence (Ru^{II} and Os^{II}) at all wavelengths to leave only the sensitized acceptor emission signal. The large difference between the quantum yields of the Ru^{II} and Os^{II} nucleosides precluded the study of 1:1 donor/acceptor duplexes. We instead monitored the steady-state emission of the Os^{II} acceptor strand in the presence of low concentrations of the complementary Ru^{II} donor strand (typically 1:10 vs acceptor strand). Even under such conditions and with D/A pairs at short distances (where energy transfer is effective), the emission spectrum is dominated by the Ru^{II} emission. Subtraction of the normalized donor signal from this spectrum gives a corrected emission spectrum identical to that of the control Os^{II} acceptor strand, indicating that under these conditions the potential sensitized emission is likely to be within the experimental error.

(26) See Supporting Information for additional data.

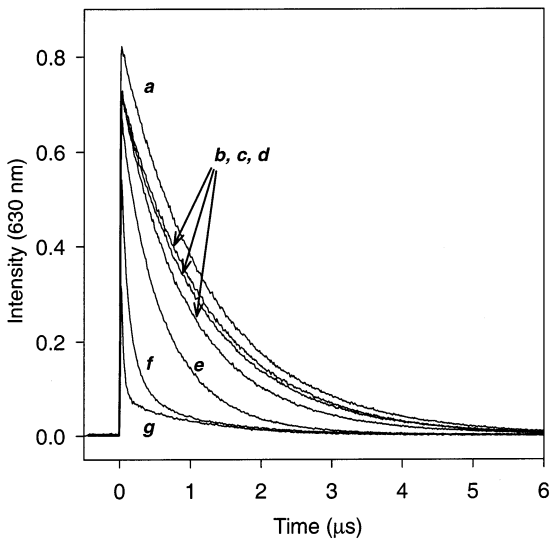

Figure 7. Time-resolved luminescence decay of the U^{Ru}(19)·Comp control duplex **5·4** (a) and the D/A oligonucleotides **5·6**−**5·11** (g−b, respectively). The luminescence decay exhibits a decrease in intensity and lifetime as a function of decreasing Ru^{II}/Os^{II} nucleotide separation (2 μM duplex concentration in degassed 100 mM NaCl, 10 mM phosphate buffer at pH 7.0).

the fraction quenched obtained in the steady-state experiments (Figure 8A).

Analysis: Förster Mechanism. The efficiency of a nonradiative Förster energy transfer decreases with increasing donor/acceptor distance (R), according to $1/[1 + (R/R_o)^6]$. R_o is the critical Förster radius, the distance at which 50% of the donor's excited-state energy is transferred to the acceptor. The magnitude of R_o depends on the spectral characteristics of the donor and acceptor complexes, as well as their relative orientation. R_o can be calculated from eq 1, where η is the refractive index of the medium separating the donor and the acceptor, κ^2 is a geometric factor associated with the relative orientation of the donor/acceptor transition dipoles, Φ_d is the quantum yield of the donor molecule in the absence of the acceptor, and J is the spectral overlap integral between donor emission and acceptor absorbance (see Figure 9).[27]

$$R_o = (8.79 \times 10^{-5}\, J\kappa^2\eta^{-4}\Phi_d)^{1/6}\ \text{Å} \qquad (1)$$

Using the photophysical characteristics of our Ru^{II}/Os^{II} system and an initial orientational parameter $\kappa^2 = {}^2/_3$, we estimate R_o to be 26 Å. A calculated Förster curve is then plotted next to the experimentally determined quenching data (Figure 10A). A significant deviation is observed. On the basis of the experimental data, an apparent R_o value of 32.5 Å is obtained. Similarly, a theoretical Förster plot of $\ln(1/E - 1)$ versus $\ln R$, where the expected slope is 6.0, shows significant difference (Figure 10B). A least-squares analysis of the experimental data gives a slope and exponential term of 3.5, indicating a shallower distance dependence than that theoretically predicted by the Förster theory.

As R_o is largely determined by the invariable photophysical characteristics of the donor and acceptor molecules, the discrepancy between the calculated value (26 Å) and the experimentally determined one (32.5 Å) is likely to result from an uncertainty in the orientation factor κ^2. κ^2 can range between 0 and 4 but typically is assigned a value of ${}^2/_3$ when the orientations of the transition dipole moments of both the donor and acceptor molecules are randomized.[28] Since the metal complexes are linked to the DNA duplex through a rigid ethynyl linker, this assumption is not valid.[29] As illustrated in Figure 10, considerably better correlations are obtained when the predicted Förster behavior is recalculated using the experimentally determined R_o value.

The deviation of certain data points from the Förster curve recalculated for $R_o = 32.5$ Å is not surprising. Since the rigidly linked Os^{II} complexes precess about the helix with increasing separation from the Ru^{II} nucleotide, *a different κ^2 value is expected for each donor/acceptor pair* (see Figure 3). Nonetheless, in view of the orientational approximations involved and on the basis of the reasonable agreement between the experimental steady-state quenching results and the corrected theoretical Förster curve (particularly for duplexes **5·7**−**5·10**, where 20 < D/A < 50 Å), it appears that the Förster mechanism can account for a significant component of the observed energy transfer. To further examine this possibility, an additional set of D/A duplexes was prepared, where the ethynyl moiety linking the Ru^{II} complex to the heterocycle has been replaced by a flexible two-carbon chain. This modification was expected to partially relax the rigid geometry of the donor chromophore, thus, bringing the orientation factor κ^2 closer to a ${}^2/_3$ value.[30]

Duplexes Containing a Saturated Ru^{II}−U Linker. Figure 11 shows a series of modified DNA duplexes that contain nucleoside **2**, where the Ru^{II} donor is linked to the heterocycle via a saturated two-carbon linker (see Figure 2).[31] This is the only structural difference that distinguishes duplexes **5·6**−**5·11** from the series **12·6**−**12·11**. The oligonucleotides' sequence is unchanged, and the complementary strands all contain the same Os^{II} complex that is linked via the unsaturated ethynyl linkage. The six bis(heterometalated) DNA duplexes are characterized by similar donor/acceptor separations of 21, 24, 34, 46, 54, and 64 Å calculated using the helical model of DNA.[32] All form stable duplexes with T_m values above 60 °C in a 10 mM phosphate buffer at pH 7.0 containing 100 mM NaCl (Table 2).

Energy transfer between the DNA bound Ru^{II} donor and Os^{II} acceptor in **12·6**−**12·11** was monitored using both steady-state and time-resolved techniques. The steady-state transfer efficiency at each of the six donor/acceptor separations was determined by comparing the integrated emission area over 500−825 nm with that of the $U^{\sim Ru}$(19)·Comp control duplex

(27) To calculate R_o for the Ru^{II} and Os^{II} D/A pair **1a**/**1b**, we used the following parameters: $\eta = 1.33$ (index refraction of water), $J = 3.9 \times 10^{-14}$ nm^6 mol^{-1} (see Figure 9), and $\Phi_d = 0.045$. See text for discussion related to the value of κ^2.

(28) This is a valid assumption when fluorophores are covalently linked to the DNA via long and flexible linkers.

(29) Anisotropy data are unlikely to provide useful information regarding the orientational restriction of the metal complexes attached to the DNA. The experimentally measured anisotropy values for our Ru^{II}-containing duplexes are extremely low (~0.006 for both the end- and internally modified duplexes), most likely because of the long lifetime of the Ru^{II} chromophore relative to the tumbling rate of the oligonucleotides.

(30) Note that saturating the linker also electronically "disconnects" the metal center and the nucleobase.

(31) See Supporting Information for the synthesis of the "saturated" Ru^{II}-containing nucleoside **2** and its phosphoramidite.

(32) The helical model of DNA for oligos containing **2** was slightly altered from that used for the **1a**/**1b** system, in that Ru^{II}/Os^{II} distance was calculated from the Ru^{II} metal center in the metalated nucleoside rather than from the carbon analogous to the thymidine 5-methyl group because of the nearly symmetrical distribution of the excited over the diimine ligands (helical parameters $a = 6$, $d = 11$, $L = 2$ Å). See Supporting Information for details.

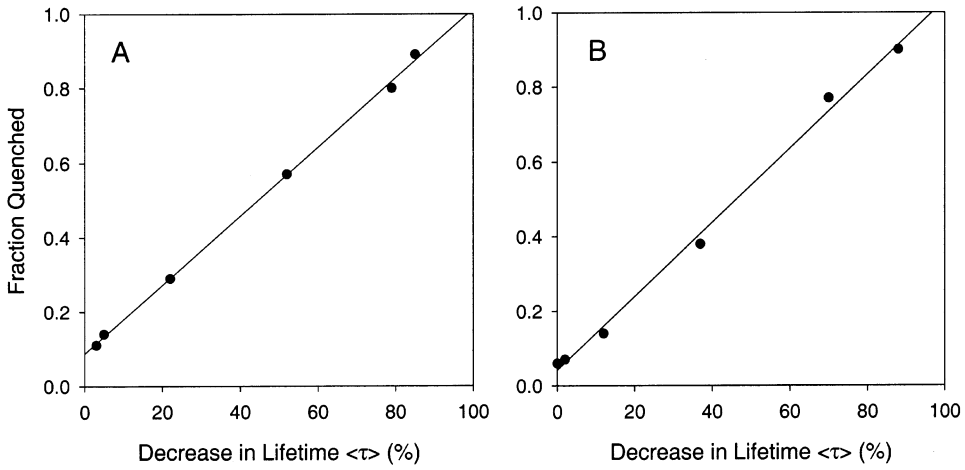

Figure 8. Excellent linear correlation is observed between the steady-state emission quenching and the decrease in the average excited-state lifetime in duplexes **5·6**−**5·11** (A) and **12·6**−**12·11** (B). In both cases, $r^2 \geq 0.995$.

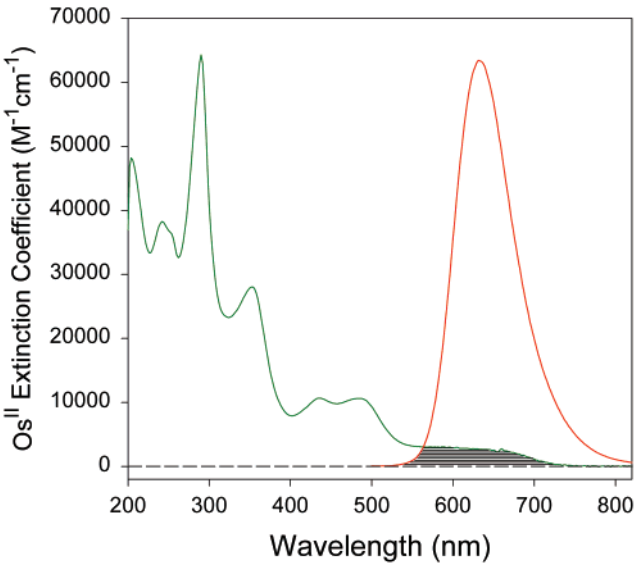

Figure 9. UV−vis absorption spectrum of the Os^{II} nucleoside **1b** (green) compared to the emission spectra of the Ru^{II} donor nucleotide in duplex U^{Ru}(19)·Comp **5·4** (red). Both are taken in aqueous solution. The region of donor/acceptor spectral overlap is shaded.

12·4.[33] The results are presented in Table 2 as the fraction quenched at each distance. As with the "unsaturated" duplex series (**5·6**−**5·11**), a decrease in quenching efficiency was observed with increasing donor/acceptor separation. The transfer efficiency decreases from a value of 90% at the shortest separation of 21 Å and levels off to ~6% quenching by 64 Å, a donor/acceptor separation of 18 base pairs.[34]

The excited-state lifetimes of the metal-modified duplexes were measured by monitoring the decay of the Ru^{II}-based emission at 607 nm and are listed in Table 2. While the decay of the Ru^{II} nucleoside **2** is monoexponential with an excited-state lifetime of 0.73 μs, the incorporation of the nucleoside into a DNA single strand **12** results in a biexponential decay, characterized by a longer-lived decay ($\tau 1 = 1.23$ μs) accompanied by a shorter-lived decay ($\tau 2 = 0.57$ μs).[35] The longer averaged excited-state lifetime, the biexponential decay, and its distribution are likely to results from random intrastrand stacking interactions with heterocyclic bases. Further support is obtained by duplex $U^{\sim Ru}$(19)·Comp (**12·4**), where the excited state is characterized by a strictly monoexponential decay with a lifetime of 0.59 μs. This suggests that the flexibly tethered Ru^{II} complex only weakly interacts with the DNA duplex, either electronically or through groove binding. The introduction of an Os^{II}-nucleoside on the complementary strand results in the modulation of the excited-state lifetime (Table 2). At the farthest Ru^{II}/Os^{II} separation (64 Å), no reduction in the excited-state lifetime is observed.[36] As before, the closer the Os^{II} quencher is to the Ru^{II} complex, the shorter the averaged Ru^{II} excited-state lifetime $\langle\tau\rangle$ (Table 2). Similarly to duplexes **5·6**−**5·11**, the decrease in the averaged excited-state lifetime for duplexes **12·6**−**12·11** is linearly correlated with the steady-state quenching results (Figure 8B).

Plotting the steady-state quenching data obtained for **12·6**−**12·11** against distance results in a sigmoidal correlation (Figure 12A). In this case, the data points fall closer to a Förster curve calculated for $\kappa^2 = {}^2/_3$ ($R_o = 24$ Å) than for the rigidly held system discussed above (Figure 10A).[37] A corrected curve recalculated for the experimentally observed R_o (31 Å) shows good correlation for distances between 20 and 55 Å (Figure 12A). Similarly, a theoretical linear Förster plot of $\ln(1/E - 1)$ versus $\ln R$, where the expected slope is 6.0 (Figure 12B), better correlates with the data when compared to the unsaturated system **5·6**−**5·11**. The observations of the duplexes containing a "relaxed" Ru^{II} donor **2** thus strongly suggest that the deviations from idealized Förster behavior observed with the duplexes containing the rigidly held Ru^{II} center **1a** originate, at least partially, from ambiguities in the orientation factor κ^2.

(33) Note that this "deconjugation" changes the photophysical properties of the Ru^{II} complex. Nucleoside **2** displays a shorter emission wavelength when compared to that of **1a** (607 vs 630 nm, respectively) and a lower quantum yield than that of **1a** ($\Phi_d = 0.042$ vs 0.045, respectively).

(34) The residual 6% quenching observed for the longest D/A separation can mainly be attributed to interduplex interactions, as demonstrated above for the soluble quencher $[(bpy)_2Os(phen)]^{2+}$ (see Figure 5A).

(35) The contribution of each decay is 50%, which is similar to the biexponential decay distributions observed in the single strands containing the conjugated nucleoside **1a**.

(36) This further supports that the 6% quenching observed at the largest D/A separation is interduplex static quenching (see ref 34 above).

(37) Note that because of the electronic change in the chromophore, the integral overlap has slightly changed and, as a result, the calculated value of R_o. The overlap integral we obtain for the **2**/**1b** system is $J = 3.8 \times 10^{-14}$ nm^6 mol^{-1}, nearly identical to the value obtained for **1a**/**1b**. The lower quantum yield and the slightly smaller overlap integral lead to a smaller calculated value of R_o (see also ref 33 above).

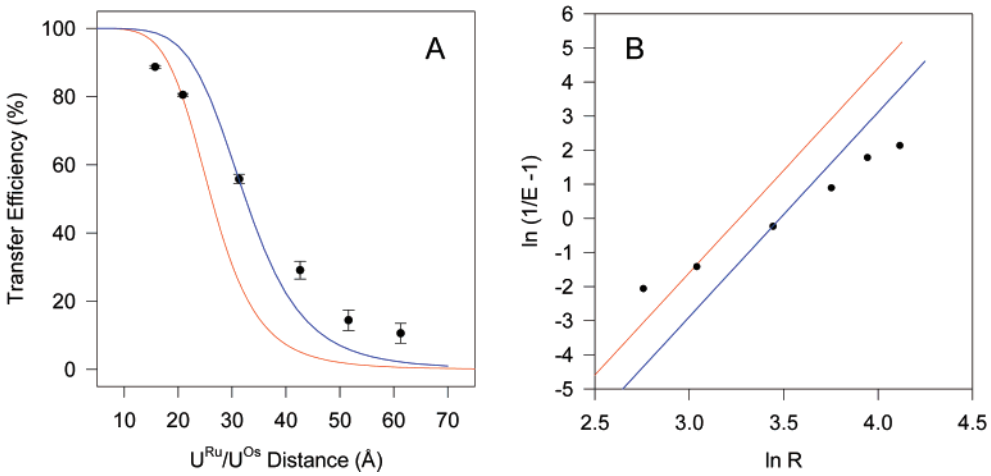

Figure 10. (A) Luminescence quenching observed for the doubly modified duplexes (**5·6**−**5·11**) plotted as a function of U^{Ru}/U^{Os} distance (calculated using the helical model of DNA; error bars represent $\pm 1\sigma$).[26] The solid lines represent the theoretical Förster curves for $R_0 = 26$ Å (red) and $R_0 = 32.5$ Å (blue). (B) log−log correlation between energy transfer efficiency and distance. The solid line represents the theoretical Förster distance dependency (slope = 6.0) for $R_0 = 26$ Å (red) and $R_0 = 32.5$ Å (blue).

Is the Dexter Mechanism Involved? The deviation of the quenching data from the idealized Förster curves warrants an evaluation of other quenching mechanisms. This is particularly imperative, since Barton has exclusively attributed observations with related Ru^{II}/Os^{II} duplexes to a triplet energy transfer mechanism.[9,38] Plotting the natural log of our experimentally determined steady-state energy transfer efficiency for duplexes **5·6**−**5·11** against distance gives a linear correlation (Figure 13).[11,39] Least-squares analysis gives a slope of -0.05 Å^{-1}, suggesting an extremely shallow distance dependency.[40] Intriguingly, an analogous "Dexter" plot for duplexes **12·6**−**12·11** also shows a linear correlation with a slope of -0.07 Å^{-1} (Figure 13). Although these respectable linear fits can be interpreted as strong evidence for a Dexter triplet energy transfer mechanism, they do not imply that this exchange mechanism is necessarily operative in these D/A duplexes. In particular, while oligonucleotides **5·6**−**5·11** may exhibit some long-range orbital coupling (because of the conjugation of the Ru^{II} center to the heterocyclic base), this is an unlikely situation for oligonucleotides **12·6**−**12·11**, where the Ru^{II} center is connected to the nucleobase via a saturated linker. The linear correlation with the Dexter model observed for both series, thus, suggests that systems that transfer energy via the Förster mechanism can under certain circumstances exhibit Dexter-like "behavior".[41,42] The satisfactory correlation of the experimental data with both the Förster and Dexter energy transfer models, particularly for duplexes **12·6**−**12·11**, illustrates the danger of imposing a single physical model to describe D/A interactions in such complex systems.

Summary

Donor/acceptor interactions have been explored in a series of oligonucleotides that contains Ru^{II} and Os^{II} nucleosides placed on complementary strands. To minimize perturbations, a single DNA sequence was utilized and only the internal positioning of the Os^{II} acceptor was adjusted. The donor/acceptor separation has been systematically varied in three base pair increments over a wide distance range (3−18 base pairs). Photoinduced energy transfer, determined by steady-state and time-resolved techniques, was analyzed according to the Förster dipole−dipole and the Dexter electron exchange mechanisms. Surprisingly, the two radically distinct mechanisms yield a reasonable correlation for duplexes containing the rigidly held Ru^{II} and Os^{II} nucleosides (duplexes **5·6**−**5·11**) as well as for duplexes that contain a flexibly linked Ru^{II} donor (duplexes **12·6**−**12·11**). We conclude that the primary mechanism responsible for mediating energy transfer in these donor/acceptor oligonucleotides is the Förster dipole−dipole interaction.[43] The extremely shallow distance dependency observed with the Dexter model for a wide distance window (D/A separation of 16 to above 60 Å) is unlikely to have a true physical meaning, as this electron exchange mechanism operates at short distances. It is difficult, however, to unequivocally exclude a minor contribution from the Dexter mechanism at short D/A distances; yet, it remains difficult to envision a physical model that brings the donor and

(38) See Supporting Information for an analysis of Barton's system (ref 9) according to the Förster energy transfer mechanism.
(39) Plotting the same data using the function utilized by Barton (ref 9), correlating $\ln(I_{Ru}/I_{RuOs} - 1)$ against distance, gives similar results.
(40) Note that this is similar to the slope Barton obtained in analyzing the data reported in ref 9.
(41) A close inspection of the time-resolved data depicted in Figure 7 shows that, at relatively large D/A separations (D/A > 30 Å), a small and constant reduction in emission intensity is observed relative to the control strand luminescence. In contrast, at shorter separations (D/A < 30 Å), this static quenching is distance dependent and much more profound, reaching approximately 55% of intensity loss at the closest chromophore separation of 16 Å. At a D/A separation of 32 Å, this intensity loss drops to 6%. A plot correlating the log of this "static" quenching efficiency versus the short D/A distances is linear (see Figure S5 in the Supporting Information). The slope of this correlation provides a measure analogous to the electronic coupling parameter β that was marked as γ by Barton (ref 9). This may suggest some involvement of triplet energy transfer in mediating D/A interactions, although it remains difficult to propose a physical model that brings the donor and the acceptor to sufficient proximity, unless partial fraying of the duplex is invoked. The loss of emission intensity and changes in the excited-state lifetime at relatively short D/A separations, therefore, suggest a complex behavior in which duplex dynamics may play an important role. Note that conformational effects on energy transfer in simple Ru^{II}/Os^{II} dyads have been observed. See: Belser, P.; von Zelewsky, A.; Frank, M.; Seel, C.; Vögtle, F.; De Cola, L.; Barigelletti, F.; Balzani, V. *J. Am. Chem. Soc.* **1993**, *115*, 4076−4086.
(42) It is interesting to add that Förster, in discussing transfer mechanisms for electronic excitation (ref 4a), demonstrates that in certain circumstances the curve for dipole−dipole energy transfer can be approximated by a simple exponential relationship.
(43) Investigating oligonucleotides that contain a bulged A or an A:C mismatch between the metal centers in both $U^{Ru}(19)\cdot U^{Os}(7)$ **5·7** and $U^{\sim Ru}(19)\cdot U^{Os}(7)$ **12·7** shows no significant changes in steady-state luminescence quenching when compared to the case of the parent doubly modified duplex (see Supporting Information). These observations further suggest that nonradiative dipole−dipole interactions mediate energy transfer in these donor/acceptor oligonucleotides.

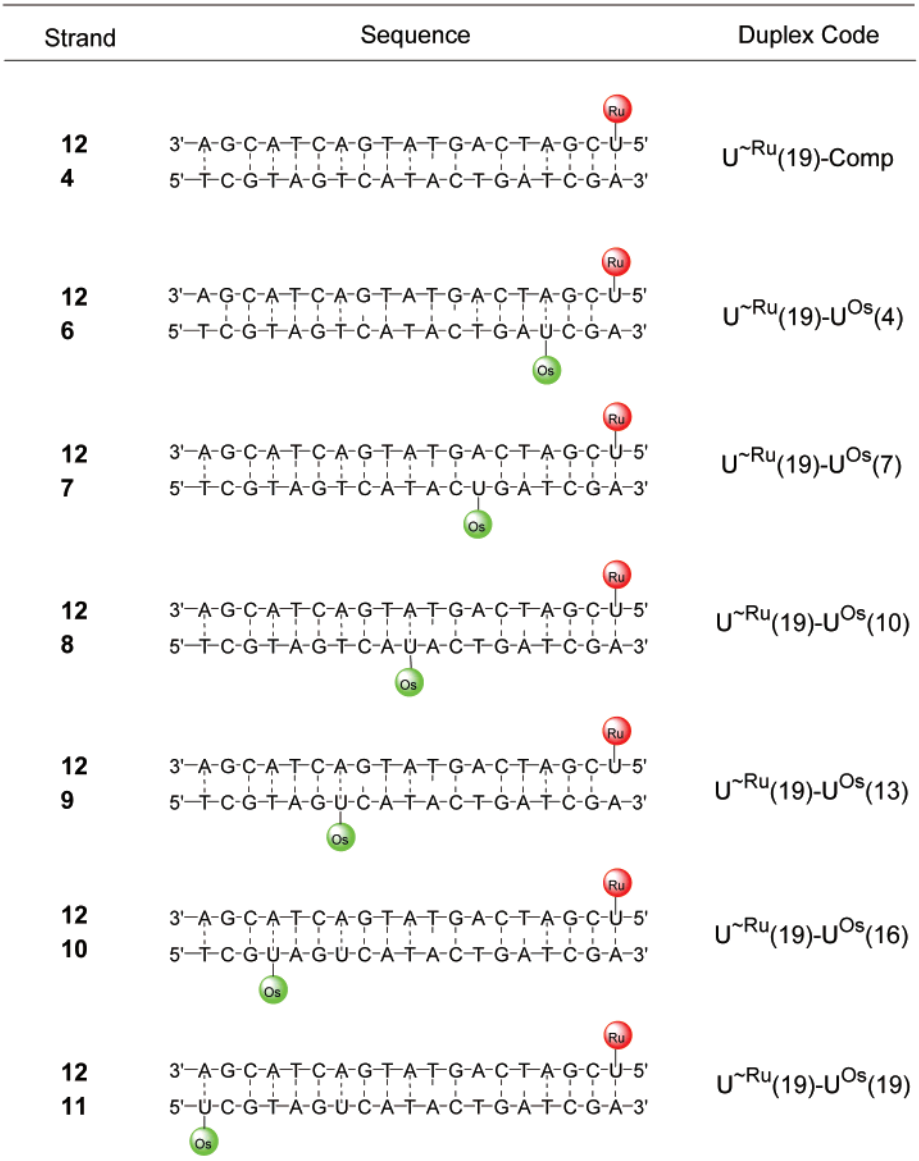

Figure 11. Six doubly metal-modified DNA 19-mer duplexes (**12·6**−**12·11**) that contain the dimethylene-linked donor Ru^{II} nucleoside **2** (red) at the 5′-end and an Os^{II} acceptor nucleoside **1b** (green) on the complementary strand. Also shown is a control oligonucleotide **12·4** and "duplex codes" which describe the D/A relationship within the duplexes in a concise manner.

acceptor to a sufficient proximity, unless temporary partial fraying of the duplex is invoked. Duplex dynamics may, therefore, play an important role in mediating such interactions and needs to be further explored. This complex behavior highlights an important feature that differentiates noncovalently assembled Ru^{II}/Os^{II} dyads from their corresponding low molecular weight, covalently attached counterparts.

Deviations from the idealized Förster behavior in duplexes **5·6**−**5·11** are illuminating. A small and constant contribution to quenching results from intermolecular interactions.[44] Notably, an accurate assessment of the orientation factor κ^2 is difficult. In this unique system, where the donor and the acceptor are rigidly held in the major groove and the orientation vector precesses around the double helix, a different κ^2 value is expected for each D/A pair. This renders the calculation of a "single" inclusive Förster curve essentially impractical. This notion has been experimentally supported by an analogous series of oligonucleotides (duplexes **12·6**−**12·11)** that contains a "relaxed" Ru^{II} donor. This modification partially "randomizes" the D/A relative orientation and brings the orientation factor κ^2 closer to a $^2/_3$ value.

Our studies with DNA-bridged D/A arrays reveal the following: (a) the DNA double helix is an intriguing platform for the study of charge transfer processes; (b) the double helix serves as an electronically indifferent scaffold for mediating dipole−dipole Förster energy transfer (particularly for D/A separation between 20 and 50 Å); (c) DNA dynamics and end effects may facilitate closer contacts between the D/A pair, leading to the possible involvement of electron exchange processes at short D/A separations; (d) comparison with idealized Förster behavior suffers from difficulties in correctly determining the orientation

(44) Note we cannot unequivocally exclude minor contributions from redox-mediated quenching processes, although unpublished results from our lab show minimal strand or sequence dependence on D/A interactions in related oligonucleotides (to be published).

Table 2. Thermal Denaturation, Steady-State Luminescence Quenching, and Excited-State Lifetimes of DNA Duplexes Containing a "Saturated" Dimethylene-linked Ru^{II} Donor **2** and an Ethynyl-linked Os^{II} Acceptor **1b**[a]

duplex	duplex code	T_m[b] (°C)	ΔT_m[c] (°C)	D/A distance[d] (Å)	fraction quenched[e]	$\tau 1$ μs[f] (%)	$\tau 2$ μs[f] (%)	$\langle\tau\rangle$ μs[g]	decrease in $\langle\tau\rangle$ (%)
3·4	control·Comp	62.5							
12·4	$U^{\sim Ru}$(19)·Comp	63.1	+0.6			0.59(100)		0.59 ± 0.01	
12·6	$U^{\sim Ru}$(19)·U^{Os}(4)	60.4	−2.1	21	0.90 ± 0.01	0.71(5)	0.03(95)	0.07 ± 0.01	88
12·7	$U^{\sim Ru}$(19)·U^{Os}(7)	61.0	−1.5	24	0.77 ± 0.01	0.65(12)	0.10(88)	0.18 ± 0.01	70
12·8	$U^{\sim Ru}$(19)·U^{Os}(10)	61.8	−0.7	34	0.38 ± 0.01	0.37(100)		0.37 ± 0.01	37
12·9	$U^{\sim Ru}$(19)·U^{Os}(13)	63.4	+0.9	46	0.14 ± 0.04	0.52(100)		0.52 ± 0.01	12
12·10	$U^{\sim Ru}$(19)·U^{Os}(16)	62.8	+0.3	54	0.07 ± 0.01	0.58(100)		0.58 ± 0.01	2
12·11	$U^{\sim Ru}$(19)·U^{Os}(19)	63.1	+0.6	64	0.06 ± 0.02	0.59(100)		0.59 ± 0.01	0

[a] All measurements were performed with 2 μM duplex solutions in 100 mM NaCl, 10 mM phosphate buffer at pH 7.0. Steady-state and time-resolved luminescence experiments were done with deoxygenated solutions.[18,19] [b] Absorbance-derived T_m values were calculated from the derivative of each thermal denaturation curve. Standard deviations are ± 0.5 °C. [c] $\Delta T_m = T_m$(metal-modified duplex) − T_m(control unmodified duplex). [d] Donor/acceptor separations were calculated using a helical DNA model.[26] [e] Fraction quenched: $Fq = 1 - I_{Ru+Os}/I_{Ru}$. The data are the average of three separate determinations. Transfer efficiency was determined by comparing the integrated emission between 500 and 825 nm of each duplex with that of the $U^{\sim Ru}$(19)·Comp control duplex **12·4**. [f] Samples were excited at 467 nm, and emission decays were monitored at 630 nm. Decays were analyzed according to the biexponential function: $I_{em}(t) = A_1\exp(-t/\tau_1) + A_2\exp(-t/\tau_2)$. [g] Weighted average lifetimes $\langle\tau\rangle$ were calculated by the equation $\langle\tau\rangle = A_1\tau_1 + A_2\tau_2$.

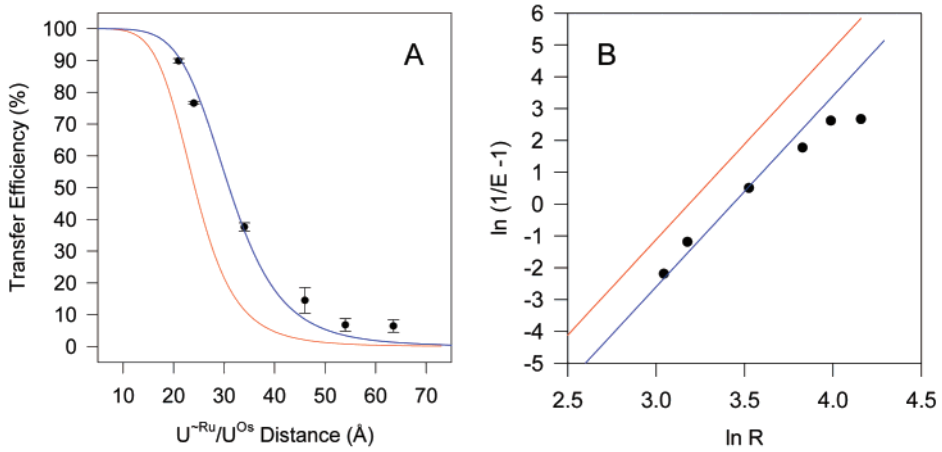

Figure 12. (A) Luminescence quenching observed for the doubly modified duplexes (**12·6**−**12·11**) plotted as a function of $U^{\sim Ru}/U^{Os}$ distance (calculated using the helical model of DNA; error bars represent ±1σ).[26] The solid lines represent the theoretical Förster curves for R_0 = 24 Å (red) and R_0 = 31 Å (blue). (B) log−log correlation between energy transfer efficiency and distance. The solid line represents the theoretical Förster distance dependency (slope = 6.0) for R_0 = 24 Å (red) and R_0 = 31 Å (blue). Note a better correlation than observed with the ethynyl-linked D/A duplexes shown in Figure 10.

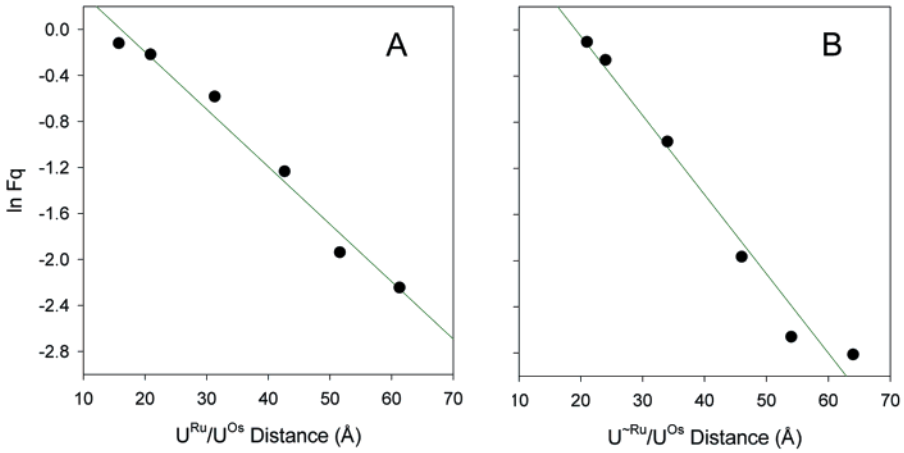

Figure 13. Plot of the distance dependence of energy transfer in duplexes **5·6**−**5·11** (A) and **12·6**−**12·11** (B) according to the Dexter mechanism. A linear correlation is obtained when the natural logarithm of the steady-state fraction quenched is plotted against distance. Least-squares analysis gives a slope of −0.05 and −0.07 $Å^{-1}$ for parts A and B, respectively.

factor κ^2; (e) polypyridine Ru^{II} and Os^{II} complexes, known to have ambiguous and complex excited-state manifolds, can participate in dipole−dipole mediated resonance energy transfer process, typically associated with "pure" singlet excited states; and (f) it is critically important to examine charge transfer processes over a large distance window to reveal the potential involvement of multiple mechanisms in mediating donor/acceptor interactions.

Experimental Section

Synthesis of Metal-Containing Phosphoramidites and Oligonucleotides. The synthesis of nucleosides **1a** and **1b** and their

corresponding phosphoramidites has previously been reported.[13,14] The syntheses of the Ru^{II}-containing nucleoside **2** and its phosphoramidite are outlined in the Supporting Information. All oligonucleotides were prepared on a 0.2-μmol scale on a 500-Å CPG solid support using a Milligen Cyclone Plus DNA synthesizer as previously reported.[13,14] Analytically pure oligonucleotides were obtained using PAGE and RP-HPLC purification. Enzymatic digestion and MS were utilized to confirm the oligonucleotide composition.[17,26]

Thermal Denaturation Studies. All hybridizations and UV melting experiments were carried out in 100 mM NaCl, 10 mM phosphate buffer at pH 7.0 containing a 1:1 ratio of complementary oligonucleotides at 2 μM duplex concentration (concentrations were evaluated by measuring the OD at 260 and 450 nm; see ref 14). After samples were prepared, they were heated to 90 °C for 5 min, cooled to room temperature for 2−3 h, and then cooled to 4 °C prior to melting temperature (T_m) measurement. Thermal denaturation studies were carried out in a Teflon-stoppered 1.0-cm path length quartz cell on a Varian-Cary 1E spectrophotometer with a temperature-controlled cell compartment. Samples were equilibrated at the starting temperature for 20 min. Heating runs were performed between 50 and 90 °C at a scan rate of 0.5 °C min^{-1} with the optical monitoring at 260 nm. All duplexes displayed sharp, two-state transition curves from duplex to single-stranded DNA. Similar results were seen in cooling curves. T_m values were determined by the computer fit of the melting data, followed by the calculation of the first derivative of the resulting melting curve. Uncertainty in T_m values is estimated to be ±0.5 °C.

Steady-State Luminescence Experiments. Steady-state luminescence experiments were conducted at 20 °C with the excitation at 467 nm on a Perkin-Elmer LS 50B luminescence spectrophotometer. Argon-degassed samples were measured at a duplex concentration of 2 μM in 100 mM NaCl, 10 mM sodium phosphate buffer at pH 7.0. Quenching efficiencies were determined by integration of the emission curves obtained from duplicated experiments on two separately prepared samples.

Time-Resolved Emission Spectroscopy. The excited-state lifetimes of the emissive complexes were measured at room temperature (22 °C) using the same samples used for the steady-state luminescence studies. The degassed solutions were excited by a 4-ns pulsed dye-laser. For duplexes containing both Os^{II} and Ru^{II}-modified nucleotides, the laser was tuned to 467 nm. At this wavelength, the ratio of the extinction coefficients for the Ru^{II} nucleoside **1a** and the Os^{II} nucleoside **1b** is 1.0 (note, however, that excitation at 450 nm yielded identical results). The emitted light was collected at 90° and focused into a monochromator. A photomultiplier tube connected to a LeCroy Digitizing Oscilloscope was used for signal detection. The data from the scope were transferred to a PC and processed using routine software of local origin. A sample of $[Ru(bpy)_3](PF_6)_2$ in acetonitrile was measured before and after each data acquisition set to ensure the stability and accuracy of the setup.

Acknowledgment. We dedicate this paper to the memory of David Sigman, a pioneer in the area of nucleic acids−metal interactions. We thank the National Institutes of Health (GM 58447) for supporting this research. We are grateful to Professor Doug Magde (UCSD) for his help and insightful comments regarding the time-resolved luminescence measurements. We also thank Dr. Hima Joshi for helpful discussions.

Supporting Information Available: Synthesis of nucleoside **2** and its phosphoramidite, enzymatic digestions of control and metalated oligonucleotides, calculation of D/A separation and the helical model of DNA, additional data regarding D/A interactions in analogous duplexes that contain bulges and mismatches, as well as a comparison to a related study by Barton. This material is available free of charge via the Internet at http://pubs.acs.org.

JA020172R